The Aigion–Neos Erineos coastal normal fault system (western Corinth Gulf Rift, Greece): Geomorphological signature, recent earthquake history, and evolution

N. Palyvos,[1] D. Pantosti,[1] P. M. De Martini,[1] F. Lemeille,[2] D. Sorel,[3] and K. Pavlopoulos[4]

Received 6 May 2004; revised 25 November 2004; accepted 13 April 2005; published 14 September 2005.

[1] At the westernmost part of the Corinth Rift (Greece), an area of rapid extension and active normal faulting, geomorphological observations reveal the existence and geometry of an active NW-SE trending coastal fault system, which includes the Aigion fault. We recognize a similar fault pattern on both the coastal range front to the NW of Aigion town and the Holocene fan deltas in front of it. We interpret this as a result of recent migration of faulting to the hanging wall of the fault system. Differences in the geomorphic expression of the constituent faults provide hints on the possible evolution of the fault pattern during this recent migration. A trench excavated across one of the identified coastal fault scarps (on a Holocene fan delta) provides information on the seismic history of the fault system, which includes at least four (possibly six) earthquakes in the past 4000 years. A minimum estimate for the slip rate of the trenched fault is 1.9–2.7 mm/yr. The trench exposed sediments of an uplifted paleolagoon (approximate age 2000 years B.P.), inside which the last two earthquakes formed an underwater monoclinal scarp. Oscillating coastal vertical movements are suggested by the fact that the lagoonal deposits are also uplifted on the trenched fault hanging wall (uplift by offshore faults) and by the abrupt transition from fluvial to lagoonal deposits (subsidence by more landward faults, assuming that extensive coastal sediment failure has not taken place in the specific part of the fan delta, within the time interval of interest). These movements suggest that the proposed migration of activity from the range front faults to those on the fan deltas is probably still ongoing, with activity on both sets of faults.

Citation: Palyvos, N., D. Pantosti, P. M. De Martini, F. Lemeille, D. Sorel, and K. Pavlopoulos (2005), The Aigion–Neos Erineos coastal normal fault system (western Corinth Gulf Rift, Greece): Geomorphological signature, recent earthquake history, and evolution, *J. Geophys. Res.*, *110*, B09302, doi:10.1029/2004JB003165.

1. Introduction

[2] The western part of the Corinth Gulf Rift in Greece (Figures 1a and 1b) is the fastest extending region in Europe and one of the fastest in the world, an area particularly well suited for the study of active normal faulting and related processes. This fact, together with high seismic hazard, has made it the target of intensive research in the past few years, a lot of which has been carried out in the frame of the Corinth Rift Laboratory (CRL) cluster of research projects [*Cornet et al.*, 2004].

[3] In this study, we adopt a geomorphological approach to obtain detailed information on the active fault pattern to the NW of the Aigion fault (AF in Figure 1c), which has been the target of many CRL activities [*Cornet et al.*, 2004]. We present observations suggesting that the Aigion fault is (or, has become) part of a substantially larger coastal fault system at the western end of the Corinth Rift. This system has been elusive due to almost complete absence of fault exposures, a complex geometry, and a subdued geomorphic signature, compared to the impressive fault escarpments of other fault systems of the Corinth Rift.

[4] We employ trenching to provide a first verification of the tectonic nature of the identified coastal scarps, as well as geological evidence of Holocene earthquakes on the fault system they comprise (which is thus shown to be active). The coastal location of the trench also allows us to explore possible relations between paleoenvironmental changes in the Holocene coastal stratigraphy and relative sea level changes (vertical movements of the coast), caused by the coastal fault system and neighboring offshore faults. The vertical movements of the coast, evaluated together with (1) the distinct fault pattern that emerges from the geomorphological observations and (2) marked differences in the geomorphic expression of the constituent faults, suggest an evolving normal fault

[1]Seismology and Tectonophysics Department, Istituto Nazionale di Geofisica e Vulcanologia, Rome, Italy.
[2]Seismic Hazard Division, Institut de Radioprotection et de Surete Nucléaire, Fontenay-aux-roses, France.
[3]Centre d'Orsay, Université Paris-Sud XI, Orsay, France.
[4]Faculty of Geography, Harokopion University, Athens, Greece.

0148-0227/05/2004JB003165$09.00

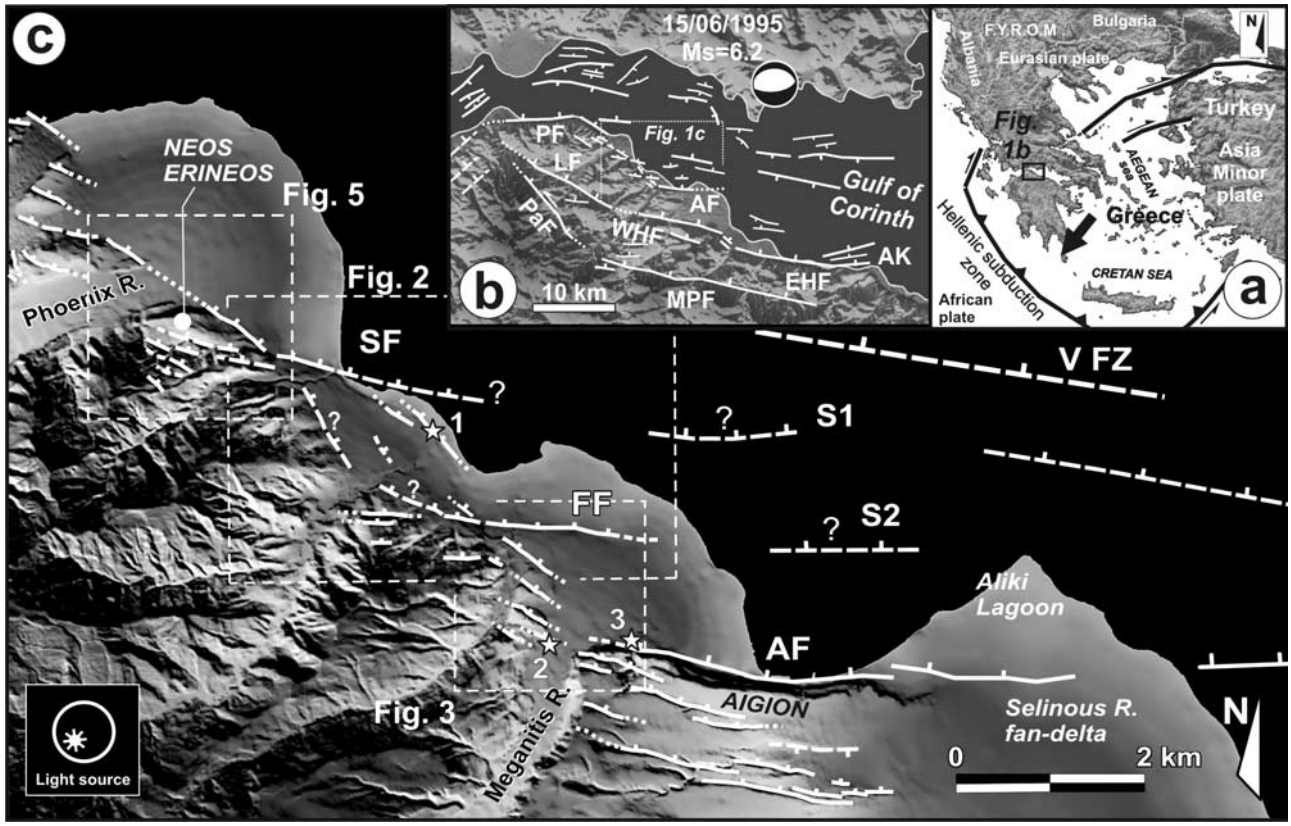

Figure 1. (a) Location map. (b) Relief and main normal fault zones of the western Corinth Gulf (ticks on downthrown side). The NW-SE coastal range front to the NW of the Aigion fault is also visible. Faults on land are from this study and *Pantosti and Palyvos* [2002] (between AF and PF) or modified from *Flotté* [2003]. Offshore faults are from *Papanikolaou et al.* [1997] and *Stefatos et al.* [2002]. Focal mechanism is from *Bernard et al.* [1997]. AF, Aigion fault; WHF, West Helike fault; EHF, East Helike fault; PF, Psathopyrgos fault; LF, Lakka fault; PaF, Panachaikon fault. (c) Shaded relief model of the study area, based on a 5-m digital elevation model (DEM) derived from 4-m contours of 1:5000 Hellenic Army Geographical Service (HAGS) topographic maps. Faults inferred based on geomorphic signature are drawn with white lines (dashed where uncertain). The pattern of E-W to ESE-WNW overlapping faults with intervening NW-SE faults is interpreted as the expression of a NW-SE fault system, which includes the Aigion fault. AF is from *Koukouvelas and Doutsos* [1996], its offshore continuation is from *Soter* [1999], and traces of offshore faults are from *Stefatos et al.* [2002]. Stars indicate paleoseismological trench locations (1, this study; 2 and 3, *Pantosti et al.* [2004]).

system and allow for hypotheses on the tendencies and possible mechanisms of its evolution.

2. Regional Setting

[5] The back arc area of the Hellenic subduction zone (Figure 1a) has been undergoing extension since the Miocene [e.g., *Kelletat et al.*, 1976; *Le Pichon and Angelier*, 1979; *Mercier et al.*, 1979]. The currently active form of the Corinth Rift has been established by rapid extension during the last 1 Ma [e.g., *Dart et al.*, 1994; *Armijo et al.*, 1996]. It has a WNW-ESE general trend and consists of roughly E-W striking, predominantly north dipping, right-stepping normal faults both on land and below sea level (Figure 1b) [e.g., *Brooks and Ferentinos*, 1984; *Doutsos and Poulimenos*, 1992; *Papanikolaou et al.*, 1997; *Moretti et al.*, 2003]. These faults accommodate extension of roughly N-S orientation [e.g., *Sebrier*, 1977; *Mercier et al.*, 1979; *Briole et al.*, 1994] and may be rooted to a low-dipping detachment at shallow (few kilometers) depth [e.g., *Melis et al.*, 1989; *Doutsos and Poulimenos*, 1992; *Bernard et al.*, 1997; *Sorel*, 2000; *Sachpazi et al.*, 2003]. Current fault activity is concentrated at the submarine part of the rift and along the southern coast of the Corinth Gulf [e.g., *Stefatos et al.*, 2002; *Avallone et al.*, 2004], where successively older faults and related depocenters are found uplifted on the footwalls of the coastal faults, reflecting a tectono-sedimentary diachronism and northward migration of fault activity [e.g., *Dufaure*, 1975; *Dart et al.*, 1994; *Sorel*, 1998; *Goldsworthy and Jackson*, 2001].

[6] The western part of the Corinth Rift is presently the most active, with geodetic extension rates reaching up to 14–16 mm/yr [e.g., *Briole et al.*, 1994, 2000; *Avallone et al.*, 2004] and intense seismicity[e.g., *Ambraseys and Jackson*, 1997; *Hatzfeld et al.*, 2000; *Lyon-Caen et al.*, 2004]. The most recent damaging event was the $M_s = 6.2$, 15 June 1995 Aigion earthquake (Figure 1b), with a focal mechanism and synthetic aperture radar solution indicating slip on a

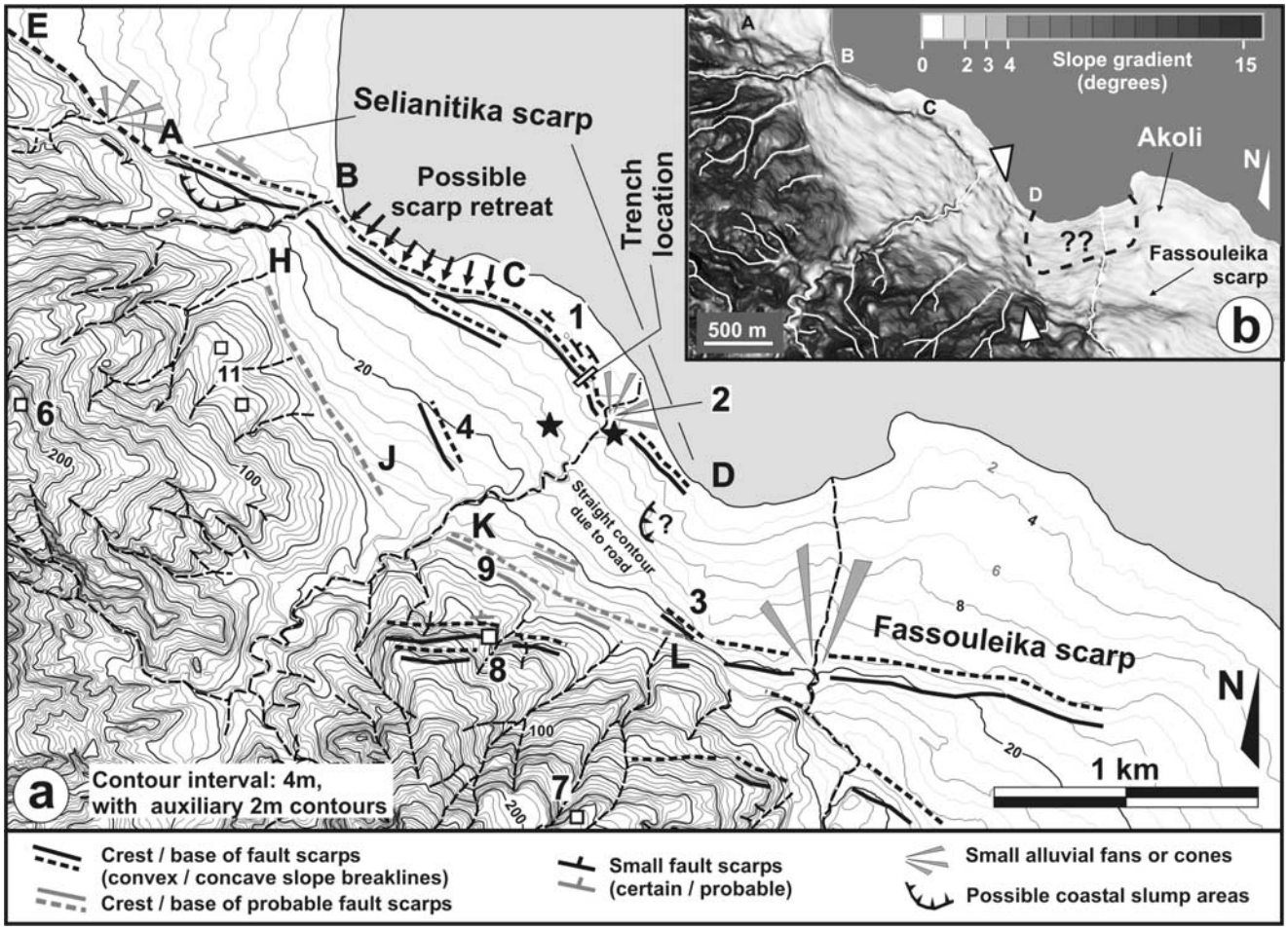

Figure 2. (a) Detailed topography and tectonic-geomorphological features of the coastal range front to the NW of the Aigion fault and the Holocene fan deltas in front of it. The prominent features on the fan deltas are the Selianitika and Fassouleika scarps. Contours every 4 m from 1:5000 HAGS topographic maps (2- and 20-m contours in gray and thicker lines, respectively). For descriptions of letters, numbered squares, and stars, see text discussion. (b) Slope model of the area based on a DEM derived from the contours in Figure 2a, plus 1-m auxiliary contours. The main coastal scarps are visible (A–D as in Figure 2a). Arrows indicate a zone across which a gentle morphological step is observed. This may be the expression of a NNW-SSE zone of small faults (not drawn in Figure 1c). A possible small slump scar along this feature is discernible (traced in Figure 2a), whereas the dashed line and the double question mark indicate a possibly larger area of coastal failure at Akoli (partially filled by a small alluvial fan) bound to the west by the NNW-SSE fault zone.

low-angle (33°) north dipping normal fault [*Rigo et al.*, 1996; *Bernard et al.*, 1997]. During this earthquake, minor surface ruptures (<4 cm vertical throw) were observed along the Aigion fault [*Koukouvelas and Doutsos*, 1996; *Bernard et al.*, 1997; *Koukouvelas*, 1998; *Lekkas et al.*, 1998]. Regardless of whether it was the 1995 seismogenic source or not, the Aigion fault is active at present, as shown by geological, paleoseismological, and geomorphological studies [e.g., *Koukouvelas*, 1998; *Lemeille et al.*, 2002, 2004a, 2004b; *De Martini et al.*, 2004; *Pantosti et al.*, 2004].

3. The Aigion–Neos Erineos Coastal Fault System

[7] The Aigion fault, for a length of 3.5 km, corresponds to a linear and steep coastal escarpment on Pleistocene fan delta deposits [*Piper et al.*, 1990; *Dart et al.*, 1994], modified by the formation of marine terraces [*De Martini et al.*, 2004]. This escarpment does not have a clear-cut continuation to the NW of the Meganitis valley (Figure 1c), yet at a broader scale, it is essentially the SE termination of a larger, NW-SE trending coastal range front that extends all the way to the Phoenix River (Figure 1c). This Aigion–Neos Erineos coastal range front (ANECR) consists of Plio-Pleistocene fan delta gravels, as well as lacustrine, brackish, and marine deposits (marls, sands, gravels). Pleistocene marine terrace remains on the ANECR [*De Martini et al.*, 2003, 2004; *Sorel and Lemeille*, 2003, and unpublished data, 2003] (e.g., at points 6, 7, and 11 in Figure 2a) suggest it has been uplifting since at least the late Pleistocene. In most of the literature it is depicted without faults at its base, with the exception of maps by *Dufaure* [1975] and *Sorel* [2000] (possible fault zone), *Flotté* [2003] (continuous fault all along it), and *Poulimenos* [1993] and *Ghisetti and Vezzani* [2004] (faults along parts of the range front base).

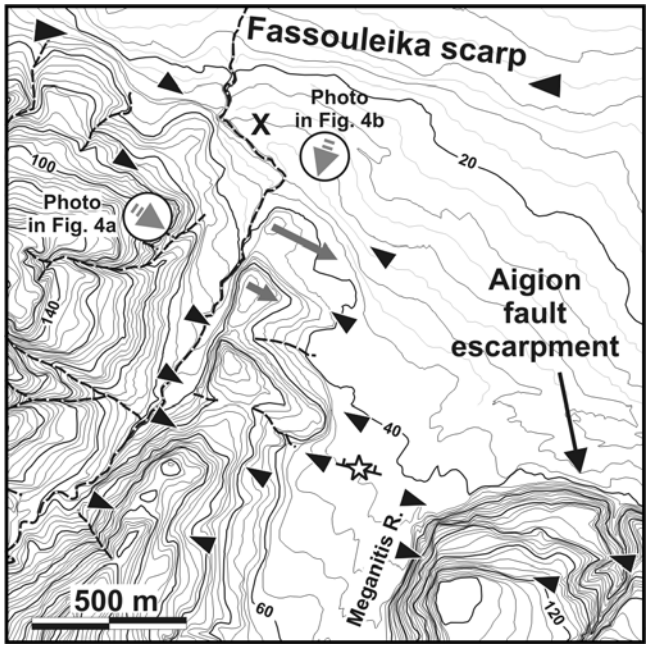

Figure 3. Detailed morphology of the coastal range front between the Aigion and Fassouleika faults (4-m contours as in Figure 2a). Small black arrows point to morphological discontinuities that are interpreted to be fault signatures (the respective faults are drawn in Figure 1c). Thick gray arrows mark the tilt direction of surfaces in between the successive faults, a configuration compliant with a relay zone. Star indicates location of the trench excavated by *Pantosti et al.* [2004] on a smaller scarp (toothed line) interrupting a late Holocene terrace of the Meganitis valley, at the prolongation of one of the inferred faults (previously mapped by *Koukouvelas and Doutsos* [1996]). Gray arrows in circles indicate the viewpoints of the photographs in Figure 4.

[8] At an even broader scale, the ANECR is itself part of a distinctly linear NW-SE stretch of coast, which we consider the expression of a NW-SE fault system in between the Aigion and Psathopyrgos faults (AF and PF in Figure 1b). Main faults belonging to this system are drawn in Figures 1b and 1c from our unpublished data (2003), partially included in the work by *Pantosti and Palyvos* [2002] (the faults collectively referred to as ''the Kamarai fault'' by *Bernard et al.* [2005]), plus newer data of this study. In this paper, we will focus on the ANECR only, discussing geomorphological observations on 1:15,000 aerial photographs from the Hellenic Army Geographical Service (HAGS), very detailed digital terrain models constructed from HAGS 1:5000-scale topographic maps (4 m contours with 1 m auxiliary ones at coastal areas), as well as geomorphological and geological observations in the field. These will be used to substantiate the presence and detailed arrangement of active faults on the Holocene fan deltas in front of, as well as on, the ANECR.

3.1. Geomorphological Signatures of Faults on the Holocene Fan Deltas Northwest of Aigion

[9] The most prominent tectonic-geomorphological features on the Holocene fan deltas NW of Aigion are two E-W to WNW-ESE trending scarps up to 15 m high, off shooting from the ANECR (Selianitika and Fassouleika, SF and FF, in Figures 1c and 2a, introduced by *Pantosti and Palyvos* [2002], *Pantosti et al.* [2004], and *De Martini et al.* [2004]). A large portion of these features has been intensely modified (motor ways and interchanges, railroad, agricultural activity, and urbanization, not depicted in Figures 1c and 2a) and their internal structure is not exposed in outcrops in the field. In Figure 2a, on the basis of maps predating a lot of the man-made modification, the Fassouleika scarp is a gentle feature traversing the Holocene fan of the Meganitis River (clearly visible in the slope model of Figure 2b). We consider it a fault scarp on the basis of (1) its straightness, (2) its direction, which is remarkably parallel to the Aigion fault, and (3) the fact that a sea cliff with such a height on the fan delta (not coinciding with a fault scarp) would imply an amount of coastal retreat which may be incompatible with the expected large sediment yield of the Meganitis River (a large river), plus coastal retreat is nowhere else associated with such a scarp in similar fan deltas from Akrata to Psathopyrgos (AK and PF in Figure 1c). Ground cracking observed along the Fassouleika scarp during the 1995 earthquake (according to people owning houses on it) may be a further indication of a subsurface discontinuity.

[10] Indications of a tectonic nature for stretches of the Selianitika scarp (A-B and C-D in Figures 2a and 2b) are (1) secondary scarps on and in front of it (synthetic or antithetic, point 1 in Figure 2a), (2) a marked stream deflection along the scarp trace (2 in Figure 2a), (3) a systematic occurrence of water wells along the scarp base, and (4) marked geochemical anomalies in the groundwater (the old sulphuric baths in the Selianitika village are near B in Figure 2a), which suggest the presence of a fault zone [*Pizzino et al.*, 2004]. Compared to the Fassouleika scarp, the Selianitika scarp is generally closer to the present shoreline and it has a more complex trace. Upon intersecting the coastline, it exhibits a marked seaward concavity in plan view (section B-C in Figure 2a), contrasting to its quite straight trace west of point B (A-B in Figure 2a). This concave stretch is also substantially steeper than the inland one (Figures 2a and 2b), suggesting that it is a coastal cliff (the fault scarp retreated) and that fault A-B is continuing offshore (probable offshore trace in Figure 1c). Detailed offshore data are not available for this area, but in a small-scale map by *Stefatos et al.* [2002], two faults (S1 and S2 in Figure 1c) are plotted roughly at the prolongation of the proposed offshore continuation of fault A-B as well as of the Fassouleika fault. These offshore faults are considered secondary structures on the footwall of a main fault further north (Valimitika fault, VF in Figure 1c; see *Stefatos et al.* [2002], also mapped earlier by *Papanikolaou et al.* [1997] with a more NW-SE trend).

[11] In between the E-W to WNW-ESE faults discussed above, we infer a number of roughly NW-SE faults based on (1) section C-D of the Selianitika scarp (the one we trenched), (2) smaller and gentle scarps identified further south (3 and 4 in Figure 2a), and (3) distinct morphological discontinuities in between the Fassouleika and Aigion Faults (Figure 3). A substantial part of scarp 3 has been modified (stone wall along it), but the original morphology is still preserved at its SE part. Scarp 4 is a very gentle but distinct feature in the topography, visible also the field. Arguments for the NW-SE faults inferred in Figure 3 are

Figure 4. Geomorphological signature of the NW-SE faults to the WNW of the Aigion fault. (a) View of the successive knickpoints created by these faults at the NW divide of the Meganitis valley. (b) View of surfaces tilted to the SE, in between the NW-SE faults. Photograph viewpoints and fault traces are indicated in Figure 3.

that (1) they correspond to straight geomorphic discontinuities, (2) they are responsible for the formation of strongly asymmetric small valleys on the higher (older) terrain they also affect, (3) they are associated to marked steps (knickpoints) on the long profile of the divide between the Meganitis River and the stream to its NW (Figure 4a), (4) distinct SE tilting of late Pleistocene surfaces is observed in between them (Figure 4b), (5) one is associated with a marked stream deflection (X in Figure 3), and (6) one is visible at an outcrop [e.g., *Koukouvelas and Doutsos*, 1996], whereas its prolongation across the Holocene terrace of Meganitis River hosted minor vertical displacements during the 1995 earthquake [*Koukouvelas and Doutsos*, 1996; *Lekkas et al.*, 1998]. Here the presence of a fault was also verified by the trench of *Pantosti et al.* [2004] (star in Figure 3).

[12] In Figure 2b, we note a NNW-SSE zone of increased slope gradients that coincides with a gentle and broad step on the fan delta surface. This may be the expression of a zone of small faults in between C-D and 3 (not drawn in Figure 1c), modified probably by small-scale slumping (possible slump scar drawn in Figure 2a). In Figure 2b we also note a quite extensive depression in the area of Akoli (partially filled by a small alluvial fan), which can be the scar of a much larger coastal failure (for examples, see *Papatheodorou and Ferentinos* [1997]), bound to the west by the faults inferred above. As a matter of fact, *Ambraseys and Jackson* [1997] report that up to 3 m of coastal subsidence occurred at Akoli (or Akuli) during an earthquake in 1888.

3.2. Geomorphological Indications of Faults on the Coastal Range Front

[13] In the Neos Erineos area (Figure 5a), the ANECR has a segmented profile, with a 100-m-high lower face, and a much higher (200 m) face to its SW (faces 1 and 2, respectively, in Figure 5b). A flat surface at around 108 m elevation is found in between these two faces, underlain by late(?) Pleistocene gravel of the Phoenix River. The morphological characteristics of face 1, namely, (1) its straightness, (2) its merging relation to stretch A-B of the Selianitika scarp (Figure 2a), and (3) its alignment with the NE boundary of the NW side of the Phoenix valley, suggest that it is a fault escarpment (fault E-A in Figure 5, mapped also by *Ghisetti and Vezzani* [2004]). The latter boundary is rather clearly fault controlled, coinciding with a straight scarp also on Holocene alluvium (GF in Figure 5a), which consists of an array of smaller right-stepping scarps (indicated by smaller arrows in Figure 5a).

[14] In the area of Figure 5a, the most populated maps of faults to our knowledge are those given by *Poulimenos* [1993, 2000], in which a number of faults trending roughly E-W and WNW-ESE are drawn. On the basis of geomorphological discontinuities and anomalies on face 2, we propose that this face is controlled by a number of WNW-ESE to NW-SE faults. Faults F1-F4 at the base of face 2 and in front of it (Figure 5a) are inferred by linear geomorphic discontinuities and the co-occurrence of (1) the anomalous course of a stream which, instead of flowing perpendicular to face 1, makes a sharp turn at point "x" in Figure 5a and attains the same direction as the Selianitika fault (AB in

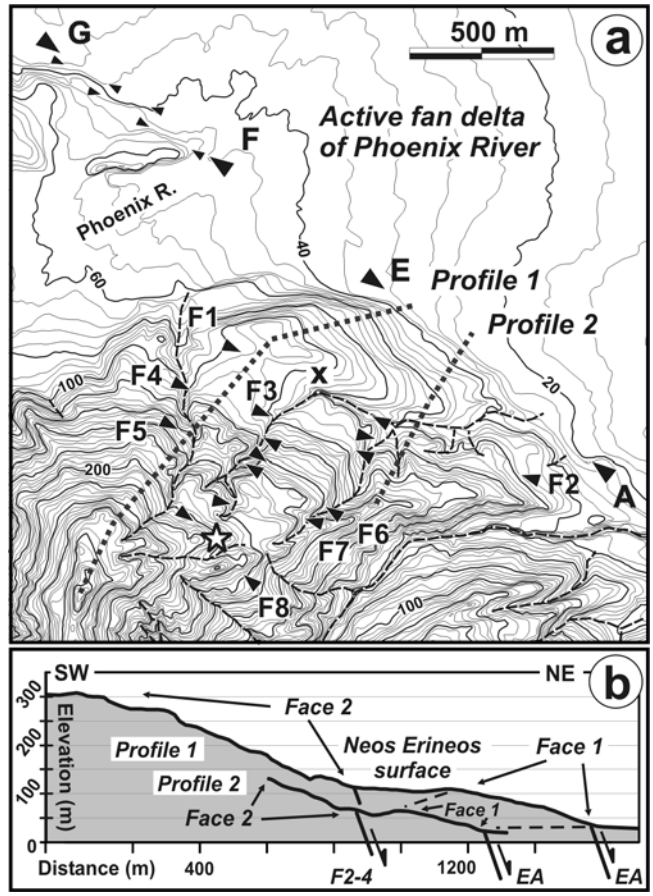

Figure 5. (a) Detailed morphology of the coastal range front in the Neos Erineos area (location in Figure 1c, 4-m contours as in Figure 2a). Small arrows point to morphological discontinuities interpreted to be fault controlled (F1–8, the respective faults are drawn in Figure 1c). Star indicates the area of fault outcrops in Figure 6. Cross indicates a fault-controlled drainage anomaly referred to in the text. Dotted lines indicate traces of topographic profiles in Figure 5b. (b) Plot of topographic profiles demonstrating the stepped morphology of the coastal range front ("stepped" not referring to small benches visible on the profile but, to the large step between faces 1 and 2).

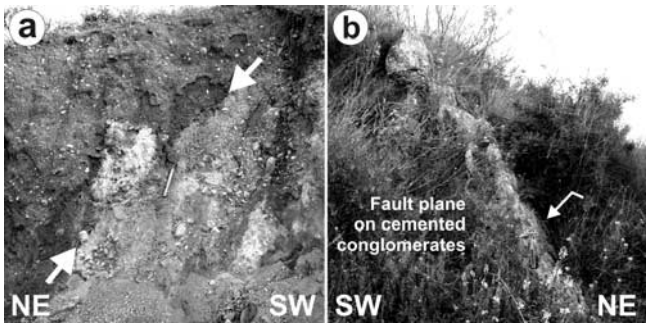

Figure 6. Views of two fault exposures on the coastal range front SW of Neos Erineos (location star in Figure 5a). (a) Fault bringing into contact Pleistocene gravel and colluvium. (b) Fault plane on cemented Pleistocene gravel.

Figure 2a) and (2) the presence of a morphological saddle NW of point 1, exactly at the prolongation of this stream, compliant with preferential erosion along a fault zone (there is no evident lithological control). On the basis of the above, we propose a zone of faults along the base of face 2 (traced with a dashed line in Figure 1c, F2-4 in Figure 5b) at the prolongation of, and with the same WNW-ESE direction as, the Selianitika fault.

[15] Face 2 is characterized by a succession of benches (Figure 5a), at least some of which may correspond to remnants of marine terraces. Yet, several narrow morphological saddles suggest possible preferential erosion along faults (e.g., lineaments F4 and F5 in Figure 5a). In general, lack of favorable outcrops hampers direct verification in the field but, in one case of appropriate exposure, faults were observed (Figure 6).

[16] At the prolongation of the Fassouleika fault to the west, we find a group of E-W scarps on the ANECR (area 8 in Figure 2a). The two main scarps are quite steep (reaching up to 30°–40°) and the elevation of their base is not constant along their length, neither does it vary in a systematic way, as we would expect should they have been cliffs behind marine terraces, or tilted marine terraces, or products of the stream to their NW. The main scarp consists of well-bedded white marls dipping generally to the SW, a fact that may be due to back tilting by a fault along it, as we propose. We found no outcrop of the inferred fault, but, a secondary zone of faulting with minor offsets can be seen at a transverse cut behind the scarp face (point 8 in Figure 2a), whereas a possible secondary scarp is found along part of the main scarp base (toothed line in Figure 2a).

[17] Around point 9 in Figure 2a, the range front morphology consists of a succession of benches separated by gentle scarps, on which the settlement of Panorama is built. This configuration may be a staircase of marine terraces, thus it will be left out of any further discussion. Yet, the straight stretch KL of the range front base (Figure 2a) can be fault controlled, judging from the relation of continuity it seems to have with the base of the Fassouleika scarp. Stretch HJ of the ANECR is straight in a NW-SE direction, with marine terrace remains on it (e.g., white squares around 11 in Figure 2a). We found no conclusive evidence of a fault zone along HJ (gentle slopes) nor scarps at its prolongation across the fan apex SE of L (Figure 2a). Still, in view of the discussion in section 8.2, we will leave the possibility of fault control open (a fault with low rates of activity in the recent past).

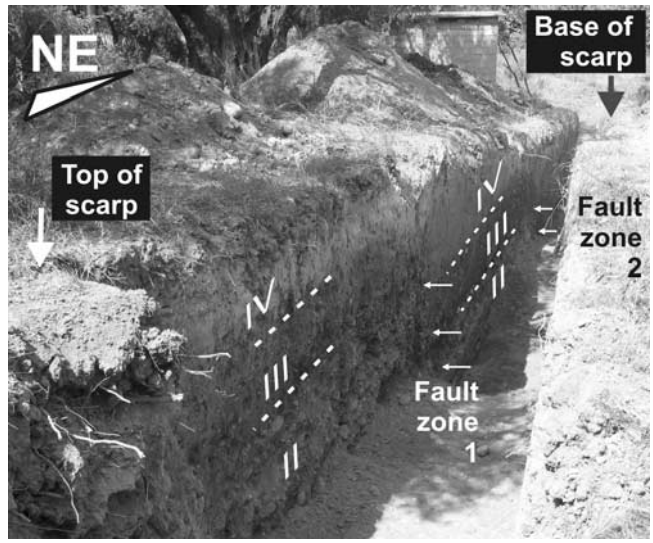

Figure 7. General view of the trench excavated across stretch C-D of the Selianitika scarp (location in Figure 2a). Discernible stratigraphic units are numbered with roman numerals (III to IV, see text and Figure 9).

4. Trench Location and Holocene Stratigraphy

[18] An exploratory trench (Figure 7) was excavated in the middle of stretch CD of the Selianitika scarp (Figure 2a). The scarp at this location is gentle, 4 m high (Figure 8) and lacks indications of important man-made modification. The trench was 21 m long, single-slot type, reaching up to 3.5 m in depth from the ground surface, just above the very shallow water table (Figure 9). Two 2-m-deep cores were taken at the hanging wall of the main fault, to extend the stratigraphic data below the trench floor. Selected samples from the trench and borehole sediments were analyzed for microfauna content and radiocarbon dated. The elevation of the trench above mean sea level was measured with a tripod-mounted Zeiss Ni5 level and stadia. Sea level is drawn as a zone in Figure 9, to account for measurement errors and a tidal range of ±30 cm.

[19] Two fault zones were exposed in the trench (F1 and F2 in Figure 9). The main one was F2, which was associated with much larger total displacement and coincided with the base of the midslope section of the surface scarp. The

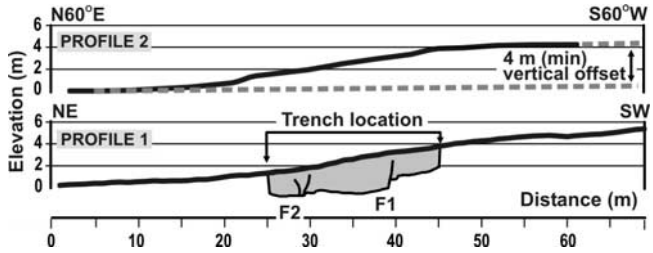

Figure 8. Topographic profiles of the trenched scarp (location in Figure 2a). Profile 1 is along the trench (drawn with gray, F1 and F2 are fault zones). Profile 2 is about 50 m to the SE of the trench.

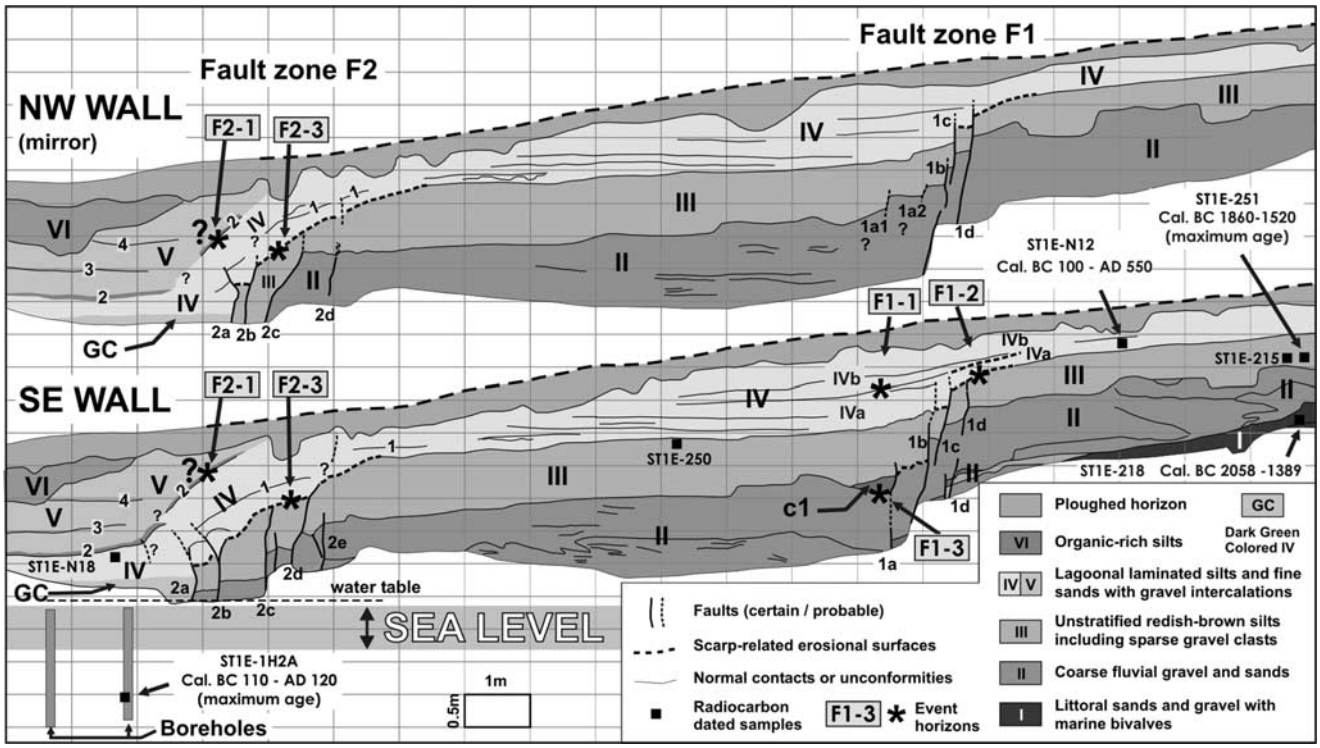

Figure 9. Logs of the two trench walls and location of the two boreholes made at the trench floor. Roman numerals and gray shades refer to main stratigraphic units, whereas layers specifically discussed in the text are numbered (1–4). Fault strands of zones F1 and F2 are labeled 1a–1d and 2a–2d, respectively. See text for correlation of paleoearthquakes between the two fault zones and for inferred events or possible events not included in this figure.

exposed stratigraphy consisted of six main units, which, numbered from older to younger (I–VI), began with a unit of coarse sands and gravel (unit I), overlain in erosional contact by coarse fluvial gravels and yellow sands (channel deposits, unit II). Unit I contained marine shells (*Patella* sp. and other bivalves), indicating a littoral environment of deposition. Unit II was overlain by an unbedded unit of oxidized silts and sparse rounded gravel clasts (unit III), which is interpreted as a subaerial deposit of slope wash and over-bank fines. Unit IV was a package of whitish-yellow finely laminated silts and fine sands. Lamination was observable only locally, whereas few bedding surfaces were discernible macroscopically, associated to rare layers of coarse sands and fine gravel. Unit IV contained an *Ostrea edulis* valve (indicating a brackish or marine environment), gastropods indicative of a low-salinity or freshwater "paludal" environment (*Viviparus* sp., smooth shell (B. Keraudren, personal communication, 2003)), as well as terrestrial gastropods (*Rumina decollata* (M. Mancini, personal communication, 2003)). This mixed macrofauna suggests a brackish environment, namely, a lagoon or, less likely, an estuary. Estuaries are typically related to mouths of large rivers [e.g., *Friedman and Sanders*, 1978], which is not really the case here. Moreover, the deposits of unit IV can be found at a substantially extensive area, judging from their appearance in small outcrops to the SW and SE of the trench (a minimum indication of their extent is given by black stars in Figure 2a).

[20] The borehole cores retrieved from the F2 hanging wall were dominated by grayish dark green silts (or clayey silts) and fine sands, including a horizon of fine gravel (clasts up to 1 cm) that contained shell fragments. A brackish depositional environment with fluctuating salinity is indicated by the microfauna found in core samples: ostracods mainly, associated in some layers with abundant benthic foraminifera (*Ammonia becarii, Elphidium* sp. and other species). A similar, abundant ostracod fauna was found in the lower horizons visible in the NE part of the trench (GC and IV) where the association of *Tyrrhenocythere amnicola*, *Cyprideis torosa,* and *Candona* sp. (larvae or fragments) with rare benthic foraminifera, indicates a low-salinity brackish water environment (C. Guernet, personal communication, 2003).

[21] We interpret the core sediments to be the continuation of the lagoonal unit IV, something that suggests a marked thickening of this unit across zone F2, due to synsedimentary faulting. Horizon GC at the bottom of the trench (grayish dark green clayey silt) is not a true stratigraphic unit but, the result of coloration of unit IV in a reducing environment, the same been probably the case for at least the top part of the boreholes, were grayish-yellow horizons were still preserved. Coloration is indicated by (1) the perfectly horizontal geometry of the top of GC, in contrast to the deformed topmost layer of unit IV above it (numbered 2 in Figure 9) and (2) its position at the exact same elevation on the two trench walls, a few centimeters above the water table (in summer), in contrast to layer 2 which is lower at the NW wall.

[22] The youngest units in the F2 hanging wall were a package of massive silts and fine sands (unit V), onlapping

Table 1. Radiocarbon Ages for Dated Samples From the Trench Across Stretch C-D of the Selianitika Scarp[a]

Sample	Lab	Material/Unit	$^{13}C/^{12}C$ Ratio, ‰	Measured R/C Age, years B.P.	Conventional R/C Age ($^{13}C/^{12}C$ Corrected), years B.P.	2σ Calibrated Age and Calibration Curve Used
ST1E-N18	Beta–181336[b]	*Viviparus* shells/unit IV	−6.4	2520 ± 40 (AMS)	2830 ± 40	1130–860 B.C. (intcal98)
ST1E-N12	Beta–181337[b]	*Ostrea* valve/unit IV	+1.7	1890 ± 40 (AMS)	2330 ± 40	100 B.C. to A.D. 100 (marine98) A.D. 350–550 (marine98 and ΔR = 380)
ST1E-1H2A	Beta–181338[b]	charred material/unit IV	−20.4	1920 ± 40 (AMS)	2000 ± 40	110 B.C. to A.D. 120 (intcal98)
ST1E-250	03S214[c]	bulk sediment/top of unit III	−22.9		4400 ± 40	3310–2900 B.C. (intcal98)
ST1E-251	03S215[c]	bulk sediment/bottom of unit III	−23.0		3390 ± 40	1860–1520 B.C. (intcal98)
ST1E-215	Beta–190269[b]	*Hellicella* shell/unit III	−8.5	4920 ± 40 (AMS)	5190 ± 40	4218–3821 B.C. (intcal98)
ST1E-218	Beta–190268[b]	*Patella* shell/unit I	+1.7	3480 ± 40 (AMS)	3920 ± 40	2058–1823 B.C. (marine98) 1571–1389 B.C. (marine98 and ΔR = 380)

[a]Calibrated with the CALIB version 4.2 software [*Stuiver and Reimer*, 1993] and calibration curves (intcal98, marine98) by *Stuiver et al.* [1998]. Sample locations are given in Figure 9. Samples ST1E-N12 and ST1E-218 are calibrated both with and without the local correction factor (ΔR = 380 years) for marine reservoir effect proposed by *Soter* [1998].
[b]Beta Analytic Inc., Miami, Florida.
[c]BRGM, France.

unit IV on the hanging wall of zone F2, and an organic-rich silt (unit VI), filling what was probably a man-made channel (in part at least), with an unusual association of large (>10 cm) pebbles and ceramic fragments at its bottom. Unit V is essentially the same type of deposits as unit IV, but four samples taken at 25 cm intervals contained practically no microfauna, although they were rich in shell fragments as the rest of the examined samples. The provenance of shell fragments is assumed to be from older (Pleistocene) deposits uplifted in the hinterland, as in the case of Holocene sediments studied in a borehole in front of the Aigion fault [*Guernet et al.*, 2003; *Lemeille et al.*, 2004a]. The position of unit V just below the surface and its onlapping relationship to the F2 footwall deposits, suggest that it was deposited by the nearby stream (2 in Figure 2a), which has created a small fan at its exit from the scarp.

5. Dating of Stratigraphic Units

[23] Dating was rather problematic, since charcoal was found only in one of the boreholes, whereas only material less suitable for radiocarbon dating was found in the trench (bivalve and gastropod shells in units I, III, and IV), together with nondiagnostic ceramic fragments. The locations of the dated samples can be seen in Figure 9, and the dating details in Table 1. The measured ages were corrected for $^{13}C/^{12}C$ fractionation and calibrated for $^{14}C/^{12}C$ changes in the atmosphere with the CALIB v. 4.2 software [*Stuiver and Reimer*, 1993]. All ages reported in the following are calibrated ages.

[24] Two *Viviparus sp.* shells (sample ST1E-N18) and transported charred material in one of the boreholes (sample 1H2A), both at the hanging wall of zone F2, yielded contradicting ages: the stratigraphically higher *Viviparus* appear older than the borehole sample (Table 1). The possibility that the borehole sample might have been roots (younger than the sediment) is considered unlikely, whereas transportation of the *Viviparus* can be safely excluded, since they were two intact shells right next to each other. Their smooth type of shell (B. Keraudren, personal communication, 2003) and a −6.4 ‰ $^{13}C/^{12}C$ ratio [*Aitken*, 1990], suggest an environment dominated by fresh water. In this context, the older age of the *Viviparus* may be attributed to hard water effect, during a period when the lagoon was dominated by fresh water. Hard water effect is a known problem in the Corinth Gulf coasts [e.g., *Soter*, 1998] due to a hinterland dominated by Mesozoic limestones.

[25] A dated *Ostrea edulis* valve (sample ST1E-N12) from the bottom of unit IV (Figure 9) yielded a $^{13}C/^{12}C$ ratio of +1.7 ‰, indicative of marine water environment [e.g., *Aitken*, 1990]. For comparison, similar ratios were obtained for gastropods from an uplifted Holocene beach by *McNeill and Collier* [2004] at a nearby fan delta (+1.2 and +0.9‰ (L. McNeill, personal communication, 2003)). This either suggests that when the *Ostrea* was living the lagoon was dominated by marine water, or that it was transported (by waves or man) into the lagoon. In any case, the age of the valve is expected to be close to the age of the surrounding deposit. On the basis of the above, we calibrate the conventional age with a marine calibration curve, thus getting an age of 100 B.C. to A.D. 100 (Table 1). If we follow *Soter* [1998] in applying a local correction factor (ΔR) of 380 years to the marine reservoir effect, the age becomes even younger (A.D. 350 to A.D. 560).

[26] In the absence of other, more suitable material, we also dated a terrestrial shell (*Helicella* sp., sample ST1E-215) and two bulk samples of sediment from the top and bottom of unit III (ST1E-250/251), apparently containing some appreciable amount of organic matter. The stratigraphically higher bulk sample was much older than the one below, suggesting substantial inclusion of reworked material. Thus we will consider the age of the lower bulk sample as a maximum for unit III (1860–1520 B.C.). The dated *Helicella* was from same level as the lower bulk sample and yielded an older age, which we consider erroneous (hard water effect?), since it is also older than the maximum possible age obtained for a *Patella* shell from unit I (ST1E-218).

6. Geological Evidence of Repeated Holocene Earthquakes

[27] On the basis of the stratigraphic and tectonic features recognized in the trench, we can obtain information on

the recent earthquake history of the trenched fault [e.g., *McCalpin*, 1996; *Yeats et al.*, 1997]. The paleoseismic evidence will be discussed for each fault zone separately, with events numbered from younger to older (F1-1 is event 1 in zone F1, F2-3 is event 3 in zone F2, etc). Subsequently, these will be summarized and correlated based on stratigraphic position.

6.1. Fault Zone 1

[28] We recognized the youngest event in fault zone 1 (F1-1) on faults 1c, 1d and 1b. Fault 1c displaces the lower part of unit IV (IVa) on both walls, the F1-1 event horizon being under unit IVb that seals the fault. Fault 1b (SE wall only) was associated with cracks and shearing of IVa, but with minor discrete displacement and perhaps a small amount of warping, whereas 1d clearly displaces the bottom of IVa on the NW wall. We found no indications of a second event during the deposition of unit IV along zone F1.

[29] A second event (F1-2), during (or after) the deposition of unit III and before the deposition of IVa, is recorded on faults 1d and 1b (both walls). Both faults are associated with larger displacement of the bottom of III compared to the bottom of IVa (IVa is not displaced at all by 1d on the SE wall and by 1b on the NW wall), whereas on fault 1d an across-fault thickness increase of unit III is observed on both walls. Event F1-2 occurred before the deposition of IVa, during (or after) the deposition of unit III. After this event some erosion of the coseismic scarp should have occurred, but no scarp-derived deposits were unequivocally identified, possibly because of the unfavorable, highly homogeneous nature of unit III.

[30] A third event back in time (F1-3) can be proposed based on fault 1a (SE wall), which displaces the top of unit II and is associated with a possible scarp-derived colluvial wedge (unit c1 in Figure 9). We did not identify a similar colluvial wedge on the NW wall, something which is probably due to the unfavorable nature of the deposits and the fact that 1a probably corresponds to two splays on this wall (1a1 and 1a2 in Figure 9), which may have produced a gentler scarp at the surface. An indirect argument that perhaps favors event F1-3 at the top of unit II is the subsequent change in depositional environment, which could be due to stream channel avulsion caused by the earthquake.

6.2. Fault Zone 2

[31] The youngest faulting in F2 (F2-1) corresponds to substantial flexuring of unit IV up to its top, which is a distinct layer of fine gravel and sand (layer 2 in Figure 9). Even if layer 2 was deposited with some initial dip (draping a paleoscarp), it seems unlikely that what we observed is its original depositional geometry. The flexure of layer 2 is accompanied by minor cracks such as along fault 2a, and essentially corresponds to an underwater monoclinal scarp [e.g., *McCalpin*, 1996]. The fact that we see no substantial warping of the contact between units II and III, reflects a different style of deformation due to different mechanical behavior of the sediments. Absence of warping of the top of horizon GC is merely due to GC not being a stratigraphic unit, but the product of postdepositional coloration, as previously discussed.

[32] In Figure 9, we put the event horizon of F2-1 on layer 2, but we add a question mark and note that the observed flexure may be the result of more than one event. This is so, because it seems unrealistic to assume that layer 2, a layer of unconsolidated fine gravel was preserved on this steep scarp face without any erosion (as suggested by the fact that no accumulation of gravel derived from layer 2 was observed at the base of the scarp). In view of this, it could be that the observed dip of layer 2 is the result of more than one earthquake, the youngest one having taken place after the deposition of unit V, which protected layer 2 from erosion. Unfortunately, bedding inside unit V was very hard to identify, and two bedding surfaces (3 and 4 in Figure 9) recognized on the basis of change in grain size could not be traced with confidence close enough to layer 2; thus we were not able to conclude whether they have been flexured against it or not.

[33] On the basis of the absence of unit III in the boreholes and assuming that this is not due to erosion, we accept that a package of IV at least 2.6 m thick is found in front of F2 (below layer 2), whereas a thickness less than half as much is observed in the warped zone. This large thickness difference implies that more than one earthquake may have occurred during the deposition of unit IV. Thus we propose a possible extra event (F2-2, no event horizon drawn in Figure 9).

[34] An older event on zone F2 (F2-3) is recognized at fault 2c, which does not affect unit IVa but displaces the bottom of unit III by 35 cm on the SE wall and more than 1.2 m on the NW wall. A change in III thickness of the same amount is also observed across the fault, suggesting faulting during or after the deposition of unit III. The 1.2 m of minimum displacement across fault 2c, predating the deposition of unit IV, could be an indication of at least one more event during the deposition of unit III also (probable event F2-4).

6.3. Summary and Timing of Events and Slip Rate Estimates

[35] On the basis of the discussed observations, the late Holocene seismic history of the trenched fault involves at least four earthquakes (E1-4), whereas two more are possible.

[36] 1. E1 took place in zone F2 (F2-1) after the deposition of unit IV. This event was associated with flexuring of unit IV underwater into a monoclinal scarp rather than discrete displacement. Accepting the age obtained from unit IV in one of the boreholes, E1 occurred sometime after 110 B.C. As discussed in section 6.2, there is a possibility that the observed flexuring may be the result of two events after the deposition of unit IV.

[37] 2. E2 occurred during the deposition of unit IV. It is evidenced in F1 and inferred in F2 by the large thickening of unit IV observed across it (events F1-1 and F2-2, respectively). E2 took place after the deposition of the lower part of unit IV (IVa) and before the deposition of its top part (IVb). On the basis of the maximum possible age for the *Ostrea* sample, E2 took place sometime after 100 B.C.

[38] 3. E3 took place during (or after) the deposition of unit III (F1-2/F2-3, evidenced on both zones). It is probable that there was more than one event during the deposition of unit III (possible event F2-4). On the basis of the maximum age for the bottom of unit III and the minimum possible age

we have for unit IV (the minimum possible age of the *Ostrea*) this event took place after 1860 B.C. and before A.D. 550.

[39] 4. E4 happened after the deposition of unit II (F1-3) and before unit III. The age obtained for unit I constrains the timing of E4 sometime after 2058 B.C. Note that we cannot use the age obtained for unit III to constrain the upper time limit for E4, since the age for unit III is a maximum age.

[40] Correlation of stratigraphic markers across both F1 and F2 not being available, we can only calculate a minimum for the vertical displacement the trenched fault has produced in the time span of the exposed deposits. This can be estimated by the minimum vertical displacement of the top of unit III, which is downthrown by at least 4 m by zone F2 (judging from its absence from the F2 hanging wall and the two boreholes and, accepting that it has not been eroded) and 1 m by zone F1. This amounts to a minimum of 5 m total vertical displacement. On the basis of the maximum age for unit III (3810 years B.P., sample ST1E-251 in Table 1), we thus derive a minimum vertical displacement rate of 1.3 mm/yr. An alternative estimate can be derived from the minimum vertical displacement deduced from the surface scarp profiles (4 m, profile 2 in Figure 8) and the age range of the *Ostrea* from unit IV (ST1E-N12 in Table 1). These figures yield a minimum of 1.9 to 2.7 mm/yr, which is our preferred value.

7. Paleoenvironmental Changes and Their Possible Tectonic Implications

[41] The oldest deposits exposed in the trench are the littoral sands and gravel of unit I. The establishment of a fluvial channel environment (unit II) over littoral deposits indicates progradation of the subaerial part of the fan delta. This can be a result of increased erosion at the hinterland, e.g., due to fires or farming. With the available data we cannot tell whether there was relative sea level change involved in the progradation and if this might have had a tectonic origin.

[42] Unit II is assumed to be a deposit of the stream presently flowing 140 m SE of the trench (Tholopotamos, Figure 2a), based on the geomorphic context, the recent age of the trench deposits and the fact that gravel of similar caliber are found in the modern channel. In time the channel course was abandoned and deposition switched to the slow accumulating colluvium and over-bank deposits of unit III, the base of which is at places clearly erosional, indicating minor channel flow on the abandoned surface after the migration of the large channel. The channel migration could be due to regular channel avulsion (typical in fans, deltas, and fan deltas); however, earthquake-induced avulsion cannot be excluded (see, e.g., *Pavlides et al.* [2004] for a discussion of such a case at the Kerynites River just east of our study area), given that one of the paleoseismic event horizons previously proposed is essentially the II/III contact.

[43] The transition between units III and IV, a change from a subaerial to a lagoonal environment, is of interest in that it suggests relative sea level rise. Was this relative sea level rise of eustatic origin or there was also subsidence of the coast involved? If so, was this subsidence of tectonic origin? What we can comment is that the transition from unit III to lagoonal deposits is abrupt, something which seems incompatible with a hypothesis of a gradual transgression by eustatic sea level rise and the migration of a barrier-lagoon system over the subaerial part of the fan delta. The same is true for a hypothesis of slow coastal subsidence due to fan delta sediment compaction. One would expect unit III to be overlain first by facies usually characterizing the inner margin of a lagoon, like fringing marsh [e.g., *Friedman and Sanders*, 1978] and not directly the facies of unit IV. This may not necessarily have to be the case, but in the closest analogue we have (geographically and in age), the Aliki lagoon of Aigion (Figure 1c), fringing marshes are indeed present [*Kontopoulos and Avramidis*, 2003].

[44] Thus, in a first approach we favor a hypothesis of episodic subsidence, presumably at a coast which already had a barrier-lagoon system north of the trench site (otherwise we would expect littoral or near-shore deposits below IV). Such episodic subsidence could be (1) tectonic, due to slip on the faults backing the fan deltas, in conjunction perhaps with shaking-induced compaction of the coastal sediments and (2) the result of failure of the fan delta sediments [e.g., *Papatheodorou and Ferentinos*, 1997]. In the latter case, the failure could be earthquake-triggered (but not necessarily), but the causative fault could also be any one of the neighboring off-shore or coastal segments.

[45] During the 1995 earthquake, liquefaction and coastal failure phenomena were observed at a comparatively restricted scale [e.g., *Lekkas et al.*, 1996], however, much larger coastal failures are known in the area, one example being the aforementioned 3 m of costal subsidence at Akoli [*Ambraseys and Jackson*, 1997]. According to *Papatheodorou and Ferentinos* [1997], the coastal subsidence during the 1861 earthquake [*Schmidt*, 1862, 1875] on the nearby Helike fault (HF in Figure 1b), or the ''drowning'' of the ancient town of Helike during the 373 BC earthquake (located on the hanging wall of the Helike fault [*Soter and Katsonopoulou*, 1999]), was caused by quite extensive coastal sediment failures (whole trees and buildings submerged). Nevertheless, not having recognized features suggestive of extensive coastal failure to the south of the trench discussed herein, in this first approach we will assign more probability to coseismic subsidence being responsible for the transition to the lagoonal deposits of unit IV.

[46] Apart from the above, the occurrence of unit IV above modern sea level suggests that it has been substantially uplifted, if we accept that Holocene sea level was never higher than present [e.g., *Fleming et al.*, 1998; *Lambeck*, 1996]. This uplift is reasonable on the fault footwall (behind F2), but unit IV is also uplifted on the hanging wall (Figure 9). This suggests coastal uplift from offshore faults (like those mapped by *Papanikolaou et al.* [1997] and *Stefatos et al.* [2002]; see traces in Figures 1b and 1c), together with regional uplift, which is generally accepted to affect all of the Corinth Gulf southern margin [e.g., *Collier et al.*, 1992; *Armijo et al.*, 1996; *Stewart*, 1996]. Similar ''oscillating'' vertical coastal movements were proposed by *Soter and Katsonopoulou* [1999] for the fan delta occupying the hanging wall of the Helike fault (HF in Figure 1b), attributed to subsidence from the latter and uplift by offshore faults. Like inferences have been

made from a borehole in front of the Aigion fault by *Lemeille et al.* [2004a, 2004b].

8. Discussion and Open Questions

[47] The fault pattern we derive from the interpretation of geomorphic features (Figure 1c) is strikingly regular. Regardless of what exactly was the initial relation of the Aigion fault with the E-W faults to its NW (e.g., kinematically interrelated faults or not [see, e.g., *Walsh et al.*, 2003]), this fault pattern suggests that the Aigion fault is now part of a NW-SE fault system composed of E-W to WNW-ESE right-stepping faults, connected by NW-SE linkage faults (or relay faults) [e.g., *Trudgill and Cartwright*, 1994; *Childs et al.*, 1995]. This is so, even if we omit features the nature of which is not well constrained by the geomorphological observations. In this case, the first group of faults includes (1) the fault that corresponds to stretch AB of the Selianitika scarp (which we call the Selianitika fault, following *Pantosti and Palyvos* [2002]) and its probable offshore continuation, (2) the Fassouleika fault, (3) the E-W faults inferred at the prolongation of faults 1 and 2 on the range front, and (4) the Aigion fault (Figure 1c). Linkage faults are (at least) (1) the fault along stretch CD of the Selianitika scarp and scarp 3 in Figure 2a and (2) the NW-SE faults to the west of the Aigion fault (Figure 3). In the latter case, the pattern of several small faults and the SE tilting that they accommodate resembles morphostructural assemblages found in breached relay zones [e.g., *Trudgill and Cartwright*, 1994; *Childs et al.*, 1995].

[48] The regularity of the overall fault pattern is in its turn a further, independent argument favoring the interpretation we propose, that is, a tectonic origin of the described geomorphic features. It also increases the possibility that faults we draw with question marks do exist after all (e.g., HJ, or the zone of faults in Figure 2b). Furthermore, it contradicts (decreases) the possibility that the scarps on the fan deltas may be due to successive slope failures at the edge of the latter. Such a scenario would also conflict with the relation of continuity between the Selianitika and Fassouleika scarps and the range front base to their WNW (fault controlled in the first case, probably also in the second). Gravitational phenomena occurring along parts of the proposed faults are, of course, something we cannot exclude and should be kept in mind when conducting paleoseismological trenching.

[49] The Aigion–Neos Erineos fault system (ANEFS) has a NW-SE general direction, roughly parallel to the main offshore fault mapped by *Papanikolaou et al.* [1997] and *Stefatos et al.* [2002]. It includes faults to the NW of the Phoenix River (not discussed herein), where a simpler surficial fault pattern is observed [*Pantosti and Palyvos*, 2002, also unpublished data, 2003] and is responsible for the formation of the NW-SE trending coastal range front between the Aigion and Psathopyrgos faults (part of which is the ANECR, Figures 1b and 1c). The NW boundary of the system is its intersection with the Psathopyrgos fault, whereas its termination to the SE can be the damage zone identified at the offshore eastern tip of the Aigion fault by *Cotterill et al.* [2004].

[50] The extension direction in the westernmost of the Corinth Gulf is N-S to N20°E [e.g., *Briole et al.*, 2000; *Avallone et al.*, 2004] and the NW-SE ANEFS is oriented oblique to this extension direction. Thus it can be a structure accommodating oblique extension with a component of sinistral horizontal movement. A question that may be addressed in future studies is whether this has to do with the observed fault pattern of right-stepping faults oriented oblique to a NW-SE primary displacement zone.

8.1. Is the Aigion–Neos Erineos Fault System a Large Earthquake Source?

[51] As confident as we may be that the Aigion fault is now part of the ANEFS, it is a fact that it is larger than the E-W faults to its NW and it can also be considered part of the regular arrays of E-W faults that typify the southern Corinth Gulf coast to its south and east (Figure 1b). What is also a fact though, is that it is located at an area of clear change in the strike of the rift faults, from an E-W, to a NW-SE general direction: apart from the ANEFS, such a change is observed also between the West Helike fault and the Lakka fault (WHF and LF in Figure 1b, respectively), whereas it is even more pronounced between the Panachaikon and Mamoussia-Pyrgaki faults (PaF and MPF in Figure 1b). Given the above, the junction between the Aigion fault and the rest of the system to the NW (the area of Figure 3) may have particular significance in terms of earthquake segmentation of the ANEFS. Being a major geometric boundary, it is a candidate to be also an earthquake segment boundary [e.g., *DePolo et al.*, 1991; *McCalpin*, 1996]. Especially if we take into account a long NE-SW fault proposed by *Poulimenos* [1993] along the Meganitis valley, all the way to the western tip of the Aigion fault (in this case this area is also a structural boundary).

[52] Whether there is an earthquake segment boundary in the area of Figure 3 or not, is a question of particular importance in terms of seismic hazard. Unfortunately, it cannot be answered with the available paleoseismological data. Previous studies by *Pantosti et al.* [2004] were conducted at (1) a trench across one of the faults to the west of the Aigion escarpment (star 2 in Figure 1c) where ground ruptures were observed during the 1995 earthquake [*Koukouvelas and Doutsos*, 1996] and (2) a preexisting artificial cut on the main trace of the Aigion fault (star 3 in Figure 1c). The latter cut yielded a minimum of 3 earthquakes in the last 8000 years for the Aigion fault, whereas the trench yielded 3 earthquakes in the last 1000 years for the NW-SE linkage fault. In the trench presented herein (star 1 in Figure 1c), we identify at least two, quite possibly three, earthquakes in the last 2000 years. These results are inconclusive because (1) the upper part of the hanging wall stratigraphy was missing at the pre-existing cut across the Aigion fault [*Pantosti et al.*, 2004] and (2) the "three events in the last 2000 years" from the trench herein can also have taken place in the last 1450 years, if we consider the minimum possible age for the sample that constrains this time interval (ST1E-N12 in Table 1) and, in any case they may have been concentrated in the last 1000 years. Furthermore, our interpretation of the abrupt transition to lagoonal deposits in the trench as a probable indication of coseismic subsidence by more landward faults, is a reminder of the possibility of different earthquakes rupturing different splays of the fault pattern we see at the surface. Thus the two trenched

faults need not necessarily record all the events occurring on the fault system.

8.2. What Does the Fault Pattern Mean in Terms of Fault System Evolution?

[53] Given that detailed offshore data and adequate subsurface profiles on the fan deltas are not available, the following discussion on the possible significance of the fault pattern can only be based on the surface observations on land.

[54] The Selianitika fault (stretch AB of the Selianitika scarp) and the Fassouleika fault (SF and FF) are located at the prolongations of faults with the same trend on the range front (F1-4 in Figure 5a and 8 in Figure 2a, respectively). Whereas SF and FF are associated with 10- to 15-m-high scarps in Holocene deposits, the scarps along F1-4 and 8 are at the base of much higher, gentle range front facets in older (Pleistocene) deposits. The morphological transition between these two types of signature is masked (modified) by erosion of the lower parts of the range front slope (by streams or formation of marine terraces), yet we can still propose that it is not gradual, but abrupt. Without subsurface data, we cannot exclude the possibility of important (kilometer scale) retreat of the range front by marine erosion, and subsequently, burial of SF and FF by the Holocene fan deltas. A point we can make though, is that the western ends of the scarps of SF and FF are junction points with faults along the range front base that we are confident about (EA in Figure 2a and fault with "X" in Figure 3). This suggests that there is structural control on the transition between the signatures of SF/FF and their counterparts on the range front.

[55] On the basis of the above, we accept as a working hypothesis that the contrast between the geomorphic signature of SF/FF and their counterparts on the range front is not due to large-scale range front retreat but, it rather suggests migration of faulting toward the fault system hanging wall. In this case, we may propose two scenarios about the possible mechanism of this migration (Figure 10). In the first one, SF and FF are parts of the range front faults that were previously overlapping (Figure 10a, top); were, largely, deactivated due to linkage (Figure 10b, top) by footwall breaching of the respective relay zones [e.g., *Trudgill and Cartwright*, 1994; *Childs et al.*, 1995]; and now are rejuvenated because of migration of strain to the system hanging wall (Figure 10d). Linkage has been hard in between the AF and FF (by the array of NW-SE faults in Figure 3) and, either soft or hard in between SF and FF, depending on whether HJ (Figure 2a) is considered a fault or not. We are tempted to comment that HJ fits perhaps too well as a fault in this scenario and the overall fault pattern.

[56] A second scenario can be that SF and FF are products of growth (off shoot) of the E-W range front faults

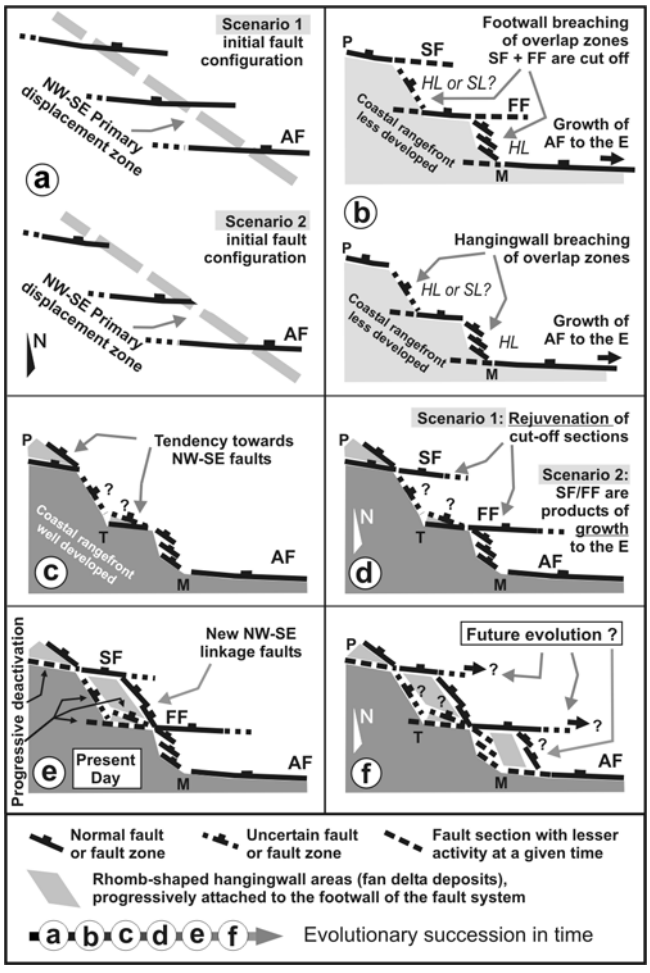

Figure 10. Scenarios for the recent evolution of the fault pattern of the studied stretch of the Aigion–Neos Erineos fault system, involving migration of faulting toward the system hanging wall. In scenario 1, the SF and FF are sections of the range front faults that were previously overlapping (Figure 10a, top) were largely deactivated due to linkage (Figure 10b, top) by footwall breaching of the respective relay zones [e.g., *Childs et al.*, 1995] and now are "rejuvenated" due to migration of strain to the system hanging wall (Figure 10d). Linkage has been hard in between the AF and FF (by an array of NW-SE faults) and, either soft or hard in between SF and FF, depending on whether HJ is considered a fault or not (see text). In scenario 2, SF and FF are products of extension (off-shoot) of the E-W range front faults toward the east. Initial fault pattern in Figures 10a (bottom) and 10b (bottom) depicts hanging wall breaching of the overlap zones (producing no cutoff sections). Growth occurs in the stage of Figure 10d, instead of rejuvenation. We note that the fault pattern in Figures 10a (top) and 10a (bottom) can be the result of earlier evolution of the system. Figure 10c depicts a possible tendency from faults trending E-W to ESE-WNW, to faults with more NW-SE directions (see text). The present-day situation is given in Figure 10e, with SF and FF cutting through the Holocene fan deltas, and NW-SE linkage faults in between them. The westward counterparts of SF and FF on the range front may be progressively dying, as strain migrates at the set of faults on the fan deltas. In Figure 10f a possible future trend of the system is speculated, with a new set of NW-SE faults linking the Aigion and Fassouleika faults, and expansion of the WNW-ESE to E-W faults toward the system hanging wall. SF, Selianitika fault; FF, Fassouleika fault; AF, Aigion fault. HL/SL, hard/soft linkage; M, T, P, Meganitis, Tholopotamos, and Phoenix rivers, respectively.

toward the east. Here we can assume a slightly different initial fault pattern with less fault overlap (Figure 10a, bottom), but at the stage of Figure 10b (bottom), the overlap zones are hanging wall breached (producing no cutoff sections). Growth occurs at the stage of Figure 10d (instead of rejuvenation).

[57] We note that the configuration assumed in Figures 10a (top) and 10a (bottom) can be in its turn the result of evolution of a previous fault pattern, difficult to determine. Faults other than those mapped herein most certainly exist on the coastal range front (e.g., a westward extension of the Aigion fault is proposed by *Poulimenos* [1993] and *Koukouvelas and Doutsos* [1996], as well as other faults) but, intense dissection by streams has masked their geomorphic signature and does not allow us to firmly infer their trace. Furthermore, we do not consider these faults as part of the recently active pattern; they belong to earlier phases of the system evolution.

[58] Fault EA along the lower range front face at Neos Erineos (Figures 5a and 5b) can be considered younger and presently more active than F1-4 along face 2. This is so, because it has developed an escarpment 100 m high in gravel that were deposited by Phoenix River at the hanging wall of zone F2-4, whereas the presently active fan delta has shifted to the hanging wall of EA. In view of the above, Figure 10c depicts a tendency from approximately E-W to more NW-SE faults, which may also be true for the Panorama area, where we observe the same transition from E-W scarps on the range front to a NW-SE trending lower part (8 and KL in Figure 2a).

[59] We may expect that in time, the rates of activity of the counterparts of SF and FF on the range front should decrease (Figure 10e, but it could also be 10d), since they are now at the system footwall, behind more active branches of the system. The observations at Neos Erineos seem to be hinting toward this direction, indicating reduced activity at faults F1-4 (Figures 5a and 5b). Figure 10e also includes the development of a new generation of NW-SE linkage faults (scarps CD and 3 in Figure 2a), breaching the overlap zone between SF and the prolongation of FF to the range front. In this case, less and less strain is expected to be accommodated by the relay zone (or linkage fault) along stretch HJ, a fact that may explain the lack of geomorphic indications of faulting along it. Yet, because the migration process is not instantaneous but gradual, both the landward faults and the newer linkage structures are expected to be active simultaneously for some time. This can be an explanation for the possible oscillating coastal vertical movements suggested by the stratigraphy of the trench across CD (section 7).

[60] A possible future situation is depicted in Figure 10f, with the western part of the Aigion fault being progressively deactivated and new NW-SE linkage faults connecting it to the FF, breaching the overlap zone in between them. A point for future subsurface investigations may be if such features are already present, but are masked by erosion and deposition by the (large) Meganitis River.

9. Conclusions

[61] Geomorphological observations reveal a strikingly regular pattern of E-W to WNW-ESE right-stepping faults (including the Aigion fault) and intervening NW-SE linkage faults, along the coastal range front between Aigion and Neos Erineos (ANECR), as well as on the fan deltas in front of it (Figure 1c). Regardless of what exactly was the initial relation of the Aigion fault to the E-W faults to its NW, the identified fault pattern suggests that it is now part of the introduced Aigion–Neos Erineos fault system (ANEFS). This system has an overall NW-SE trend and continues also to the NW of the Phoenix River, all the way to the Psathopyrgos fault (Figure 1b). The ANECR lacks clear-cut fault escarpment morphology due to the geometrical complexity of the system (zigzag pattern), relatively soft footwall lithologies, and the development of marine terraces.

[62] The configuration on the coastal range front, with roughly E-W right-stepping faults and NW-SE (to NNW-SSE) linkage faults or relay zones in between them, appears to be repeating on the Holocene fan deltas in front of it. Accepting that large-scale coastal retreat is unlikely, we interpret this as an indication of migration of faulting toward the hanging wall of the system, via an evolutionary mechanism, that may involve (1) rejuvenation of fault sections previously cutoff in overlap zones or (2) growth of E-W faults toward the hanging wall (Figure 10). In both scenarios, newer NW-SE linkage faults develop.

[63] A trench excavated across one of the NW-SE coastal fault scarps (Figure 9, location in Figure 2a) produced evidence of synsedimentary faulting in subaerial fan delta deposits and a blanketing unit of lagoonal deposits. Oscillating coastal vertical movements are suggested by the fact that the deposits of the identified paleolagoon are uplifted on both the footwall and hanging wall of the trenched fault (uplift by offshore faults) and by an abrupt transition from a subaerial to a brackish environment (possible subsidence by landward faults, accepting that extensive coastal sediment failure has not taken place in the specific part of the fan delta, in the time interval of interest). These movements can be reflections of an ongoing process of migration of activity from the faults at the ANECR to those on the Holocene fan deltas in front of it. Since this migration is not instantaneous, all these faults can be simultaneously active for a certain period (proportional to the spatial scale of this migration).

[64] As far as the recent seismic history of the trenched fault is concerned, it involves at least four, probably six, earthquakes since 4000 years B.P., the last two having occurred in the past 2100 years. During the two most recent earthquakes surface faulting was underwater, the last one producing a characteristic monoclinal scarp. A minimum of 1.9–2.7 mm/yr vertical displacement rate is calculated for the specific fault. The presently available paleoseismological data [*Pantosti et al.*, 2004; this study] are not detailed enough to establish the presence or not of an earthquake segment boundary at the western termination of the Aigion fault, which is an important geometrical, and possibly also a structural, boundary within the ANEFS.

[65] **Acknowledgments.** We gratefully acknowledge the contributions of B. Keraudren and M. Mancini (malacofauna identification) and C. Guernet, C. Bourdillon, and M. Triantaphyllou (ostracod and foraminifera analyses). We also warmly thank L. McNeill for sharing data on radiocarbon datings of marine shells in the Corinth Gulf and J. Walsh for his comments and ideas on the evolution of the fault pattern. The

manuscript benefited substantially from the reviews and comments of R. Collier, P. Collins, and I. Stewart, whom we sincerely thank. We are also very thankful to C. Papantonopoulos, who gave permission to excavate in his lemon orchard; the vice major of the Sympoliteia Municipality, T. Sotiropoulos for his support and endorsement; IGME for work permits; the Patras Ephorate of Antiquities for the excavation permission and, the personnel of the Aigion archaeological office for their help and cooperative spirit. This work was funded by INGV (Roma), CNRS-INSU in the frame of GDR Corinth, IRSN, and the Corinth Rift Laboratory (CORSEIS project).

References

Aitken, M. J. (1990), *Science-Based Dating in Archaeology*, Longman, New York.

Ambraseys, N. N., and J. A. Jackson (1997), Seismicity and strain in the Gulf of Corinth (Greece) since 1694, *J. Earthquake Eng.*, *1*, 433–474.

Armijo, R., B. Meyer, G. C. P. King, A. Rigo, and D. Papanastassiou (1996), Quaternary evolution of the Corinth Rift and its implications for the late Cenozoic evolution of the Aegean, *Geophys. J. Int.*, *126*, 11–53.

Avallone, A., P. Briole, A.-M. Agatza-Balodimou, H. Billiris, O. Charade, C. Mitsakaki, A. Nercessian, K. Papazissi, D. Paradissis, and G. Veis (2004), Analysis of eleven years of deformation measured by GPS in the Corinth Rift Laboratory area, *C. R. Geosci.*, *336*(4/5), 301–311, doi:10.1016/j.crte.2003.12.007.

Bernard, P., et al. (1997), The M_s = 6.2, June 15, 1995 Aigion earthquake (Greece): Evidence for low angle normal faulting in the Corinth Rift, *J. Seismol.*, *1*, 131–150.

Bernard, P., et al. (2005), Seismicity, deformation and seismic hazard in the western rift of Corinth: New insights from the Corinth Rift Laboratory (CRL), *Tectonophysics*, in press.

Briole, P., J. C. Ruegg, H. Lyon-Caen, A. Rigo, K. Papazissi, G. Veis, D. Hatzfeld, and A. Deschamps (1994), Active deformation of the Gulf of Corinth, Greece: Results of repeated GPS surveys between 1990 and 1993, *Ann. Geophys.*, *12*, C65.

Briole, P., A. Rigo, H. Lyon-Caen, J. Ruegg, K. Papazissi, C. Mitsakaki, A. Balodimou, G. Veis, D. Hatzfeld, and A. Deschamps (2000), Active deformation of the Corinth Rift, Greece: Results from repeated GPS surveys between 1990 and 1995, *J. Geophys. Res.*, *105*(B11), 25,606–25,626.

Brooks, M., and G. Ferentinos (1984), Tectonics and sedimentation in the Gulf of Corinth and the Zakynthos and Kefallinia channels, western Greece, *Tectonophysics*, *101*, 25–54.

Childs, C., J. Watterson, and J. J. Walsh (1995), Fault overlap zones within developing normal fault systems, *J. Geol. Soc. London*, *152*, 535–549.

Collier, R. E. L., M. R. Leeder, R. J. Rowe, and T. C. Atkinson (1992), Rates of tectonic uplift in the Corinth and Megara basins, central Greece, *Tectonics*, *11*, 1159–1167.

Cornet, F., P. Bernard, and I. Moretti (2004), The Corinth Rift Laboratory, *C. R. Geosci.*, *336*(4/5), 235–441, doi:10.1016/j.crte.2004.02.001.

Cotterill, C., L. McNeill, A. Stefatos, T. Henstock, J. Bull, R. Collier, G. Papatheodorou, A. Georgiopoulou, and G. Ferentinos (2004), A high-resolution geophysical survey of extensional faulting (and associated features): A case study from the offshore western Gulf of Corinth, Greece, *Geophys. Res. Abstr.*, *6*, 359, SRef-ID:1607-7962/gra/EGU04-A-00359.

Dart, C. J., R. E. L. Collier, R. L. Gawthorpe, J. V. A. Keller, and G. Nichols (1994), Sequence stratigraphy of (?)Pliocene-Quaternary synrift, Gilbert-type fan deltas, northern Peloponnesos, Greece, *Mar. Pet. Geol.*, *11*, 545–560.

De Martini, P. M., N. Palyvos, and D. Pantosti (2003), Detailed mapping of raised late Pleistocene terraces between Aigion and Psathopyrgos faults and preliminary estimates of uplift rates, paper presented at Second Aegion Workshop, Corinth Rift Lab., Aegion, Greece, 3–7 June.

De Martini, P. M., D. Pantosti, N. Palyvos, F. Lemeille, L. McNeill, and R. Collier (2004), Slip rates of the Aigion and Eliki faults from uplifted marine terraces, Corinth Gulf, Greece, *C. R. Geosci.*, *336*(4–5), 325–334, doi:10.1016/j.crte.2003.12.006.

DePolo, C., D. Clark, B. Slemmons, and A. Ramelli (1991), Historical surface faulting in the Basin and Range province, western North America: Implications for fault segmentation, *J. Struct. Geol.*, *13*, 123–136.

Doutsos, T., and G. Poulimenos (1992), Geometry and kinematics of active faults and their seismotectonic significance in the W Corinth-Patras rift (Greece), *J. Struct. Geol.*, *14*, 689–699.

Dufaure, J.-J. (1975), Le relief du Peloponnese, thése d'état, 1422 pp., Univ. Paris–Sorbonne (Paris IV), Paris.

Fleming, K., P. Johnston, D. Zwartz, Y. Yokoyama, K. Lambeck, and J. Chappel (1998), Refining the eustatic sea-level curve since the Last Glacial Maximum using far- and intermediate-field sites, *Earth Planet. Sci. Lett.*, *163*, 327–342.

Flotté, N. (2003), Caracterisation structurale et cinematique d'un rift sur detachement: Le rift de Corinthe–Patras, Grece, thése doctorat, 196 pp., Univ.-Paris Sud XI, Orsay, France.

Friedman, G. M., and J. E. Sanders (1978), *Principles of Sedimentology*, 792 pp., John Wiley, Hoboken, N. J.

Ghisetti, F., and L. Vezzani (2004), Plio-pleistocene sedimentation and fault segmentation in the Gulf of Corinth (Greece) controlled by inherited structural fabric, *C. R. Geosci.*, *336*(4/5), 243–249, doi:10.1016/j.crte.2003.12.008.

Goldsworthy, M., and J. Jackson (2001), Migration of activity within normal fault systems: Examples from the Quaternary of mainland Greece, *J. Struct. Geol.*, *23*, 489–506.

Guernet, C., F. Lemeille, D. Sorel, C. Bourdillon, C. Berge-Thierry, and M. Manakou (2003), Les ostracodes et le Quaternaire d'Aigion (Golfe de Corinthe, Gréce), *Rev. Micropaleontol.*, *46*, 73–93, doi:10.1016/S0035-1598(03)00013-8.

Hatzfeld, D., V. Karakostas, M. Ziazia, I. Kassaras, E. Papadimitriou, K. Makropoulos, N. Voulgaris, and C. Papaioannou (2000), Microseismicity and faulting geometry in the Gulf of Corinth (Greece), *Geophys. J. Int.*, *141*, 438–456.

Kelletat, D., G. Kowalczyk, B. Schroder, and K. Winter (1976), A synoptic view on the neotectonic development of the Peloponnesian coastal regions, *Z. Dtsch. Geol. Ges.*, *127*, 447–465.

Kontopoulos, N., and P. Avramidis (2003), A late Holocene record of environmental changes from the Aliki lagoon, Egion, north Peloponnesus, Greece, *Quat. Int.*, *111*, 75–90, doi:10.1016/S1040-6182(03)00016-8.

Koukouvelas, I. (1998), The Egion fault, earthquake-related and long-term deformation, Gulf of Corinth, Greece, *J. Geodyn.*, *26*(2–4), 501–513.

Koukouvelas, I., and T. Doutsos (1996), Implications of structural segmentation during earthquakes: The 1995 Egion earthquake, Gulf of Corinth, Greece, *J. Struct. Geol.*, *18*(12), 1381–1388.

Lambeck, K. (1996), Sea-level change and shoreline evolution in Aegean Greece since upper Palaeolithic time, *Antiquity*, *70*(169), 588–611.

Lekkas, E., S. Lozios, E. Skourtsos, and H. Kranis (1996), Liquefaction, ground fissures and coastline change during the Egio earthquake (15 June 1995: central-western Greece), *Terra Nova*, *8*, 648–654.

Lekkas, E. L., S. G. Lozios, E. N. Skourtsos, and H. D. Kranis (1998), The Egio earthquake (15 June 1995): An episode in the neotectonic evolution of Corinthiakos Gulf, *J. Geodyn.*, *26*(2–4), 487–499.

Lemeille, F., D. Sorel, C. Bourdillon, C. Guernet, M. Manakou, and C. Berge-Thierry (2002), Quantification de la déformation associée à la faille active d'Aigion (Golfe de Corinthe, Grèce) par l'étude des dépôts du Pléistocène supérieur et de la transgression marine Holocéne, *C. R. Geosci.*, *334*, 497–504.

Lemeille, F., F. Chatoupis, M. Foumelis, D. Rettenmaier, I. Unkel, L. Micarelli, I. Moretti, C. Bourdillon, C. Guernet, and C. Müller (2004a), Recent syn-rift deposits in the hangingwall of the Aigion fault, *C. R. Geosci.*, *336*, 425–434, doi:10.1016/j.crte.2003.11.009.

Lemeille, F., P. Thierry, and D. Sorel (2004b), Interprétation géologique du profil sismique realisé par IRSN dans le port d'Aigion: Évolution paléogéographique locale (Golfe de Corinthe, Grèce Centrale), technical note, Inst. de Radioprot. et de Sûreté Nucl., Clamart et Fontenay-aux-Roses, France.

Le Pichon, X., and J. Angelier (1979), The Hellenic arc and trench system: A key to the neotectonic evolution of the eastern Mediterranean area, *Tectonophysics*, *60*, 1–42.

Lyon-Caen, H., P. Papadimitriou, A. Deschamps, P. Bernard, K. Makropoulos, F. Pacchiani, and G. Patau (2004), First results of the CRLN seismic network in the western Corinth Rift: Evidence for old-fault reactivation, *C. R. Geosci.*, *336*(4/5), 343–351, doi:10.1016/j.crte.2003.12.004.

McCalpin, J. P. (1996), *Paleoseismology*, 588 pp., Elsevier, New York.

McNeill, L. C., and R. E. L. Collier (2004), Uplift and slip rates of the eastern Eliki fault segment, Gulf of Corinth, Greece, inferred from Holocene and Pleistocene terraces, *J. Geol. Soc. London*, *161*, 81–92.

Melis, N. S., M. Brooks, and R. G. Pearce (1989), A microearthquake study in the gulf of Patras region, western Greece, and its seismotectonic interpretation, *Geophys. J.*, *98*, 515–524.

Mercier, J., N. Delibassis, A. Gauthier, J.-J. Jarrige, F. Lemeille, H. Philip, M. Sébrier, and D. Sorel (1979), La neotectonique de l'Arc Égéen, *Rev. Geol. Dyn. Geogr. Phys.*, *21*, 67–92.

Moretti, I., D. Sakellariou, V. Lykousis, and L. Micarelli (2003), The Gulf of Corinth: An active half graben?, *J. Geodyn.*, *36*, 323–340, doi:10.1016/S0264-3707(03)00053-X.

Pantosti, D., and N. Palyvos (Eds.) (2002), The Eliki and Aigion faults database (1.0), final report, EC Corseis project, Ist. Naz. di Geofis. e Vulcanol., Rome. (Available at http://www.ingv.it/~wwwpaleo/pantosti/aigion/database/)

Pantosti, D., P. M. De Martini, I. Koukouvelas, L. Stamatopoulos, N. Palyvos, S. Pucci, F. Lemeille, and S. Pavlides (2004), Paleoseismo-

logical investigations across the Aigion fault (Gulf of Corinth, Greece), *C. R. Geosci.*, *336*(4–5), 335–342, doi:10.1016/j.crte.2003.12.005.

Papanikolaou, D., G. Chronis, V. Lykoussis, D. Sakellariou, and I. Papoulia (1997), Neotectonic structure of the western Corinth Gulf and geodynamic phenomena of the Aigion earthquake, paper presented at the Fifth National Symposium on Oceanography and Fisheries, Kavala, Greece.

Papatheodorou, G., and G. Ferentinos (1997), Submarine and coastal sediment failure triggered by the 1995 M_s = 6.1 R Aegion earthquake, Gulf of Corinth, Greece, *Mar. Geol.*, *137*, 287–304.

Pavlides, S., I. Koukouvelas, S. Kokkalas, L. Stamatopoulos, D. Keramydas, and I. Tsodoulos (2004), Late Holocene evolution of the East Eliki fault, Gulf of Corinth (central Greece), *Quat. Int.*, *115–116*, 139–154, doi:10.1016/S1040-6182(03)00103-4.

Piper, J., T. Doutsos, and L. Stamatopoulos (1990), Quaternary history of the gulfs of Patras and Corinth, Greece, *Z. Geomorphol.*, *34*(4), 451–461.

Pizzino, L., F. Quattrocchi, D. Cinti, and G. Galli (2004), Fluid geochemistry along the Eliki and Aigion seismogenic segments, *C. R. Geosci.*, *336*(4/5), 367–374, doi:10.1016/j.crte.2003.11.012.

Poulimenos, G. (1993), Tectonics and sedimentation in the western Corinth graben, Greece, *Neues Jahrb. Geol. Palaeontol. Monatsh.*, *10*, 607–630.

Poulimenos, G. (2000), Scaling properties of normal fault populations in the western Corinth graben, Greece: Implications for fault growth in large strain settings, *J. Struct. Geol.*, *22*, 307–322.

Rigo, A., H. Lyon-Caen, R. Armijo, A. Deschamps, D. Hatzfeld, K. Makropoulos, P. Papadimitriou, and I. Kassaras (1996), A microseismic study in the western part of the Gulf of Corinth (Greece): Implications for large-scale normal faulting mechanisms, *Geophys. J. Int.*, *126*, 663–688.

Sachpazi, M., C. Clement, M. Laigle, A. Hirn, and N. Roussos (2003), Rift structure, evolution and earthquakes in the Gulf of Corinth from reflection seismic images, *Earth Planet. Sci. Lett.*, *216*, 243–257, doi:10.1016/S0012-821X(03)00503-X.

Schmidt, J. (1862), Sur le grand tremblement de terre qui a eu lieu en Gréce le 26 Décembre 1861, *C. R. Hebd. Seances Acad. Sci.*, *54*, 669–671.

Schmidt, J. (1875), *Studien uber Erdbeben*, 324 pp., Carl Scholtze, Leipzig, Germany.

Sebrier, M. (1977), Tectonique recente d'une transversale a l'arc egéen: Le Golfe de Corinthe et ses régions périphériques, thése doctorat, 137 pp., Univ. Paris-Sud XI, Orsay, France.

Sorel, D. (1998), Tectono-sedimentary evolution of the Quaternary Corinth–Patras rift (Greece), paper presented at the Joint Meeting on Rapid Coastal Changes in the Late Quaternary: Processes, Causes, Modelling, Impacts on Coastal Zones, Int. Geosci. Programme, Corinth and Samos, Greece, 10–19 Sept.

Sorel, D. (2000), A Pleistocene and still-active detachment fault and the origin of the Corinth–Patras Rift, Greece, *Geology*, *28*(1), 83–86.

Sorel, D., and F. Lemeille (2003), Tilting of the Aigion block in the stepover between the Psathopyrgos and Helike active faults (Gulf of Corinth, Greece) recorded by marine terraces, paper presented at the Second Aegion Workshop, Corinth Rift Lab., Aegio, Greece, 3–7 June.

Soter, S. (1998), Holocene uplift and subsidence of the Helike delta, Gulf of Corinth, Greece, in *Coastal Tectonics*, edited by I. S. Stewart and C. Vita-Finzi, *Geol. Soc. Spec. Publ.*, *146*, 41–56, PII:S0040-1951(99)00090-6.

Soter, S. (1999), Macroscopic seismic anomalies and submarine pockmarks in the Corinth-Patras Rift, Greece, *Tectonophysics*, *308*, 275–290.

Soter, S., and D. Katsonopoulou (1999), Occupation horizons found in the search for the ancient Greek city of Helike, *Geoarchaeology*, *14*(6), 531–563.

Stefatos, A., G. Papatheodorou, G. Ferentinos, M. Leeder, and R. Collier (2002), Seismic reflection imaging of active offshore faults in the Gulf of Corinth: Their seismotectonic significance, *Basin Res.*, *14*, 487–502.

Stewart, I. (1996), Holocene uplift and paleoseismicity on the Eliki fault, western Gulf of Corinth, Greece, *Ann. Geophys.*, *39*(3), 575–588.

Stuiver, M., and P. J. Reimer (1993), Extended 14C database and revised CALIB radiocarbon calibration program, *Radiocarbon*, *35*, 215–230.

Stuiver, M., P. J. Reimer, E. Bard, J. W. Beck, G. S. Burr, K. A. Hughen, B. Kromer, F. G. McCormac, J. v. d. Plicht, and M. Spurk (1998), INTCAL 98 radiocarbon age calibration, *Radiocarbon*, *40*, 1041–1083.

Trudgill, B., and J. Cartwright (1994), Relay-ramp forms and normal fault linkages, Canyonlands National Park, Utah, *Geol. Soc. Am. Bull.*, *106*, 1143–1157.

Walsh, J. J., W. R. Bailey, C. Childs, A. Nicol, and C. G. Bonson (2003), Formation of segmented normal faults: A 3D perspective, *J. Struct. Geol.*, *25*, 1251–1262, PII:S0191-8141(02)00161-X.

Yeats, R., K. Sieh, and C. Allen (1997), *The Geology of Earthquakes*, 568 pp., Oxford Univ. Press, New York.

P. M. De Martini, N. Palyvos, and D. Pantosti, Seismology and Tectonophysics Department, Istituto Nazionale di Geofisica e Vulcanologia, Via di Vigna Murata 605, I-00143 Rome, Italy. (palyvos@ingv.it)

F. Lemeille, Seismic Hazard Division, Institut de Radioprotection et de Surete Nucléaire, B.P. 17, F-92262 Fontenay-aux-roses Cedex, France.

K. Pavlopoulos, Faculty of Geography, Harokopion University, 70 El. Venizelou Str., GR-17671 Athens, Greece.

D. Sorel, Centre d'Orsay, Université Paris-Sud XI, F-91405 Orsay Cedex, France.